

# Overcoming Weak Visual-Textual Alignment for Video Moment Retrieval

Minjoon Jung<sup>1</sup> Youwon Jang<sup>2</sup> Seongho Choi<sup>2</sup> Joochan Kim<sup>2</sup>  
Jin-Hwa Kim<sup>3,4\*</sup> Byoung-Tak Zhang<sup>1,2,3\*</sup>

<sup>1</sup>IPAI & <sup>2</sup>CSE & <sup>3</sup>AIIS, Seoul National University <sup>4</sup>NAVER AI Lab

## Abstract

*Video moment retrieval (VMR) identifies a specific moment in an untrimmed video for a given natural language query. This task is prone to suffer the weak visual-textual alignment problem innate in video datasets. Due to the ambiguity, a query does not fully cover the relevant details of the corresponding moment, or the moment may contain misaligned and irrelevant frames, potentially limiting further performance gains. To tackle this problem, we propose a background-aware moment detection transformer (BM-DETR). Our model adopts a contrastive approach, carefully utilizing the negative queries matched to other moments in the video. Specifically, our model learns to predict the target moment from the joint probability of each frame given the positive query and the complement of negative queries. This leads to effective use of the surrounding background, improving moment sensitivity and enhancing overall alignments in videos. Extensive experiments on four benchmarks demonstrate the effectiveness of our approach.*<sup>1</sup>

## 1. Introduction

Video moment retrieval (VMR) [10] retrieves the target moment in an untrimmed video corresponding to a natural language query. A successful VMR model requires a comprehensive understanding of videos, language queries, and correlations to predict relevant moments precisely. In contrast to traditional action localization tasks [37, 46] that predict a fixed set of actions like “throwing” or “jumping,” VMR is a more difficult task requiring joint comprehension of semantic meanings in video and language.

A video is typically composed of short video clips, where query sentences describe each clip. However, query sentences are often ambiguous as to whether they fully express the events occurring within the matching moment, and boundary annotations might include frames unrelated to the query sentences [14, 57]. As shown in Figure 1 (top), the

moment prediction can be imprecise and weakly aligned with annotations. For instance, the query “Person pours some water into a glass” does not describe an event for “drink water”, but the boundary annotation includes it. Furthermore, queries like “Person sitting on the sofa eating out of a dish” may confuse the model, as the actions “sitting” and the object “sofa” overlap throughout the video.

Traditional VMR methods [9, 23, 28, 49, 51, 52, 54] take a single query as input to predict the moment. However, solely relying on a single query may learn only local-level alignment and hinder achieving successful VMR due to the weak alignment problem. Whereas, contrastive learning-based methods [6, 20, 29, 42] learn the query and the ground-truth moment features close to each other while keeping others apart [30]. Nevertheless, due to semantic overlap and sparse annotation dilemma [49] in videos, Li et al. [20] claimed that adopting vanilla contrastive learning into VMR is suboptimal. Negative queries from random videos used to have semantic overlap, making them false negatives, while negative moments also likely are false negatives due to the sparse annotation. This often leads to inaccurate estimation of marginal distribution used in contrastive methods of InfoNCE [30]. To overcome this, Li et al. [20] employs geodesic distance to measure semantic relevance between video moments correctly, but they still need to sample a large number of negative moments, resulting in high computational costs to approximate the true partition faithfully and achieve sophisticated alignment.

In this paper, we propose a novel **Background-aware Moment DETection TRansformer** (BM-DETR) based on the transformer encoder-decoder architecture [41]. Our encoder utilizes contexts outside of the target moments (*i.e.*, negative queries) along with the positive query. We use the probabilistic frame-query matcher to calculate the joint probability of each frame given a positive query and the complement of negative queries, resulting in frame attention scores for enhancing multimodal representations. By considering the relative relationships between queries within the video, the model learns how to best identify and focus on the relevant visual features of the target moment, improving *moment sensitivity*, or *true positive rate*. Then,

\* Corresponding authors.

<sup>1</sup>Our code is available at: <https://github.com/minjoong507/BM-DETR>

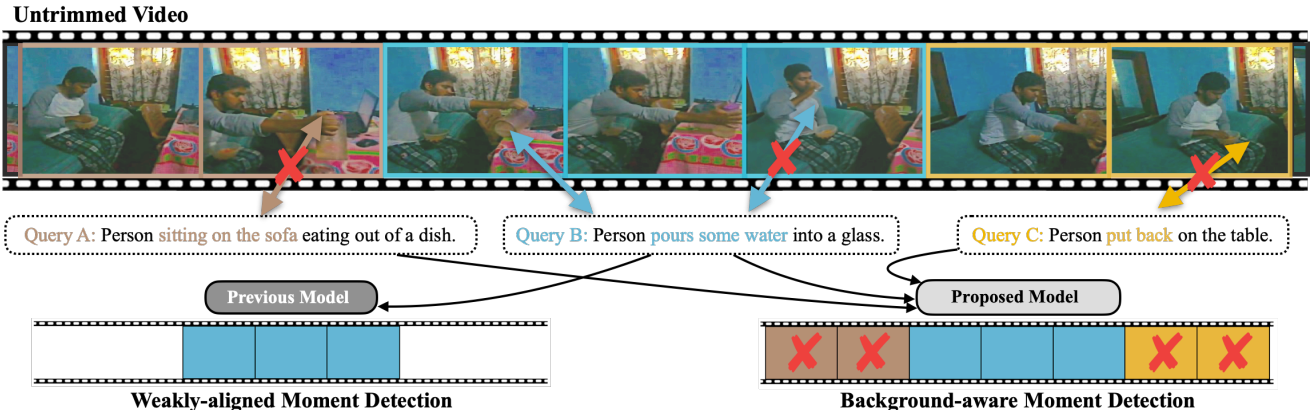


Figure 1. *Top*: An example of weak visual-textual alignment. *Bottom*: Comparison between current (left) and proposed (right) approaches.

we utilize cross-modal discrimination between other video-query pairs to learn semantic alignment. Finally, our decoder generates predictions from multimodal features using learnable spans. In addition, we leverage the temporal shifting method to improve the model’s robustness.

In contrast to previous approaches, which relied on a single query with complex multimodal reasoning or mining a multitude of negative moments with high cost, our model can attend to the target moment and be aware of the contextual meanings throughout the video, as shown in Figure 1 (*bottom*). Moreover, our method is simple and more efficient than previous contrastive methods by eliminating dense moment features and reducing redundant computations. Our model shows significant performance gains on four public VMR benchmarks: Charades-STA [10], ActivityNet-Captions [17], TACoS [33], and QVHighlights [19]. In addition, we provide out-of-distribution (OOD) testing and empirical qualitative analysis to show that our model effectively handles the weak alignment problem. To sum up, the contributions of our paper can be summarized as follows:

- We propose BM-DETR to address the weak visual-textual alignment problem, which is crucial in video moment retrieval tasks.
- By considering relative temporal and contextual relationships within videos, our model can enhance overall alignment in videos and enable robust moment detection.
- Comprehensive quantitative and qualitative analyses on four datasets demonstrate the effectiveness of our model.

## 2. Related Work

**Video moment retrieval.** Video moment retrieval (VMR) aims to retrieve the target moment in a video based on a natural language sentence. Existing approaches are mainly classified into proposal-based methods and proposal-free methods. The proposal-based methods [1, 4, 9, 10, 42, 43, 54, 55] sample candidate moments from the video and se-

lect the most similar moment to the given query. In contrast, proposal-free methods [5, 13, 23, 28, 36, 47, 49, 51, 52] regress target moments from video and language features without generating candidate moments. Recently, several studies [2, 19, 21, 22, 25, 27] utilized the framework of DETR [58] for localization tasks. While these studies have shown promising results, they have not thoroughly tackled the issue of weak alignment in videos. In this paper, our emphasis is on designing a model that effectively addresses the weak alignment problem in videos.

**Visual-textual alignment problem in videos.** Labeling videos is expensive and cumbersome, making it difficult to build high-quality and scalable video datasets. This often leads to alignment issues, which have been observed [11, 16, 26] as a crucial bottleneck of video understanding. VMR is also sensitive to these issues since it requires accurate temporal moment locations, and several studies [6, 14, 20, 29, 57] are related to these problems. To mitigate uncertainties in annotations, Zhou et al. [57] augment the phrases (e.g., verb) in language queries to improve semantic diversity, and Huang et al. [14] propose a sophisticated moment matching method. However, since they still follow traditional VMR methods, the weak alignment problem may hinder them from achieving successful VMR. In contrastive learning approaches, Nan et al. [29] introduce the causality-based model to diminish spurious correlations between videos and queries. Li et al. [20] propose a geodesic-guided contrastive learning scheme to reflect semantic relevance between video moments correctly. In this work, we propose a more effective method to mitigate the weak alignment problem while maintaining efficiency.

## 3. Method

We give an overall architecture of the BM-DETR in Figure 2. In this section, we first briefly review our task. Then, we discuss the main idea of background-aware moment detection and describe the details of our model architecture

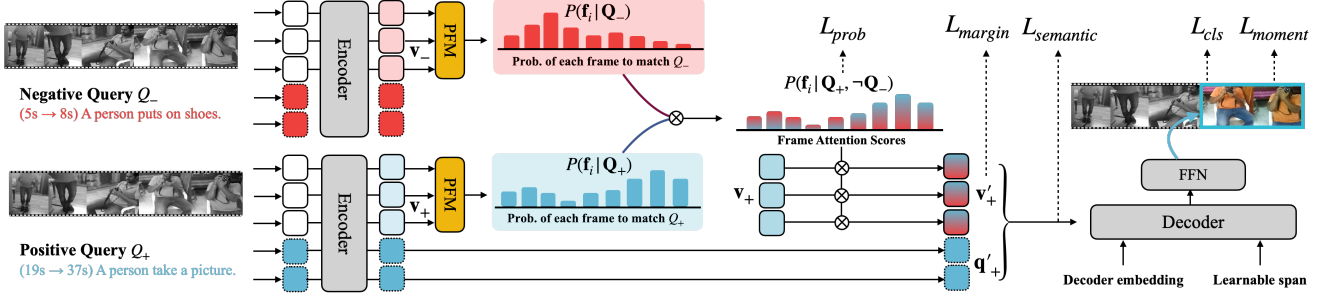


Figure 2. An overview of our BM-DETR framework. First, our encoder extracts multimodal features from given inputs. Then, we obtain frame attention scores for updating multimodal features. Finally, to complete VMR, our decoder predicts the target moment, and we calculate the losses from the prediction and ground-truth moment.

for employing it. In Section 3.4, we introduce the temporal shifting method that encourages the model’s time-equivariant predictions. Finally, we describe how our model generates the predictions for given inputs and provide details of loss.

### 3.1. Video Moment Retrieval

Given an untrimmed video  $V$  and language query  $Q$ , we represent the video as  $V = \{f_i\}_{i=1}^{L_v}$  where  $f_i$  denotes the  $i$ -th frame. Likewise, the language query is denoted as  $Q = \{w_i\}_{i=1}^{L_w}$  where  $w_i$  denotes the  $i$ -th word.  $L_v$  and  $L_w$  indicate the overall count of frames and words, respectively. We aim to localize the target moment  $m = (t_s, t_e)$  in  $V$  from  $Q$ , where  $t_s$  and  $t_e$  represent the start and end times of the target moment, respectively.

### 3.2. Background-aware Moment Detection

As mentioned earlier, a single query may not be sufficient to disambiguate the corresponding moment due to the weak alignment problem in videos. That said, predicting the target moment in  $V$  based solely on information from  $Q$  is less informative and ineffective, where the term “information” refers to the knowledge or cues used for accurate predictions of the target moment in  $V$ . Hence, we propose an alternative to resolve this problem inspired by *importance sampling* [39]. Similar to the contrastive learning [30], a specific query  $Q_+$  is designated as the target (positive), while we randomly sampled a negative query  $Q_-$  for each training. Our main idea is based on two guiding principles:

**Principle 1.** *Queries from the same video  $V$  allow for disambiguation of the target query  $Q_+$ , as they have implicit contextual and temporal relationships with the corresponding video moments.*

**Principle 2.** *To avoid spurious correlations, we differentiate between negative query  $Q_-$  and target query  $Q_+$  based on their temporal locations and semantic similarity. We use  $Q_-$  that has less intersection over union (IoU) with  $Q_+$  than a certain threshold (e.g. 0.5). Additionally, we remove  $Q_-$  that have high semantic similarity with  $Q_+$  using*

SentenceBERT [34] to reduce semantic overlap further. We will address the impact of these processes in Section 4.4.

Let  $P(f_i | Q_+)$  and  $P(f_i | Q_-)$  to be the likelihood of  $i$ -th frame to match the positive and negative queries, respectively. We assume these likelihoods are independent, as their corresponding moments are at different temporal locations, and their semantic meanings are dissimilar. Our model predicts the target moment by the joint probability of each frame, and the probability can be represented as:

$$P(f_i | Q_+, -Q_-) := P(f_i | Q_+) \cdot (1 - P(f_i | Q_-)). \quad (1)$$

Considering  $P(f_i | Q_-)$ , our model can focus on relatively more important meanings included in the target query, improving *moment sensitivity*. As we will see in the later experiments, being aware of contexts surrounding the target moment is more informative for the model’s prediction, improving further accuracy.

### 3.3. Architecture

#### 3.3.1 Encoder

Our encoder aims to catch the multimodal interaction between video  $V$  and query  $Q$ . Initially, the pre-trained feature extractor (e.g., CLIP [32]) is employed to convert each input into multi-dimensional features and normalize them. We utilize two projection layers to convert input features into the same hidden dimension  $d$ . Each projection layer consists of several MLPs. Then, we obtain video representations as  $\mathbf{V} \in \mathbb{R}^{L_v \times d}$  and query representation as  $\mathbf{Q} \in \mathbb{R}^{L_w \times d}$ . Note that there are two query representations  $\mathbf{Q}_+$  and  $\mathbf{Q}_-$  for positive and negative queries, respectively. We direct them to the multimodal encoder  $E(\cdot)$ , a stack of transformer encoder layers denoted as:

$$E(\mathbf{V}, \mathbf{Q}) = E(PE(\mathbf{V}) \parallel \mathbf{Q}), \quad (2)$$

where  $PE$  means the positional encoding function [41],  $\parallel$  indicates the concatenation on the feature dimension. Finally, we obtain multimodal features  $X_+$  and  $X_-$  represented as:

$$X_+ = E(\mathbf{V}, \mathbf{Q}_+), \quad X_- = E(\mathbf{V}, \mathbf{Q}_-), \quad (3)$$

where  $X_+$ ,  $X_- \in \mathbb{R}^{L \times d}$ , and we denote the length of concatenated features as  $L = L_v + L_w$ .

### 3.3.2 Implementing the Background-aware Moment Detection

Let us redefine the frame parts of the multimodal features  $X_+$  and  $X_-$  as  $\mathbf{v}_+ = \{\mathbf{f}_i^+\}_{i=1}^{L_v}$  and  $\mathbf{v}_- = \{\mathbf{f}_i^-\}_{i=1}^{L_v}$ , respectively. We compute the likelihood of each frame to match the positive and negative queries, denoted as  $P(\mathbf{f}_i | \mathbf{Q}_+)$  and  $P(\mathbf{f}_i | \mathbf{Q}_-)$ , respectively. These probabilities can be obtained through the **Probabilistic Frame-Query Matcher** (PFM) defined as:

$$P(\mathbf{f}_i | \mathbf{Q}_+) = \text{PFM}(\mathbf{f}_i^+), \quad P(\mathbf{f}_i | \mathbf{Q}_-) = \text{PFM}(\mathbf{f}_i^-). \quad (4)$$

PFM consists of two linear layers followed by tanh and sigmoid ( $\sigma$ ) functions defined as:

$$\text{PFM}(\mathbf{f}_i) = \sigma(\tanh(\mathbf{f}_i \mathbf{W}_1) \mathbf{W}_2), \quad (5)$$

where  $\mathbf{W}_1 \in \mathbb{R}^{d \times \frac{d}{2}}$  and  $\mathbf{W}_2 \in \mathbb{R}^{\frac{d}{2} \times 1}$  are learnable matrices. The joint probability of  $i$ -th frame  $\mathbf{p}_i$  can be calculated according to equation 1 as follows:

$$P(\mathbf{f}_i | \mathbf{Q}_+, -\mathbf{Q}_-) = P(\mathbf{f}_i | \mathbf{Q}_+) \cdot (1 - P(\mathbf{f}_i | \mathbf{Q}_-)). \quad (6)$$

After that, the softmax function is applied to obtain the frame attention scores  $\mathbf{o}$ :

$$\mathbf{o} = \text{Softmax}(\mathbf{p}_1, \mathbf{p}_2, \dots, \mathbf{p}_{L_v}). \quad (7)$$

Finally, we leverage  $\mathbf{o}$  to enhance the positive frame features  $\mathbf{v}_+$  in  $X_+$  to  $\mathbf{v}'_+$ . This can be formulated as follows:

$$\mathbf{v}'_+ = \mathbf{o} \otimes \mathbf{v}_+, \quad (8)$$

where  $\otimes$  is an element-wise product. We denote the updated multimodal features as  $X'_+$  and send it to the decoder to predict the target moment.

### 3.3.3 Fine-Grained Semantic Alignment

After encoding multimodal features, we focus on improving semantic alignment between video-query pairs. Let the visual and textual representations from the multimodal features  $X'_+$  are  $\mathbf{v}' \in \mathbb{R}^{L_v \times d}$  and  $\mathbf{q}' \in \mathbb{R}^{L_v \times d}$ , respectively. We first adopt an attentive pooling to extract the global context of each representation as:

$$\hat{\mathbf{v}} = \sum_{n=1}^{L_v} \mathbf{a}_n^v \mathbf{v}'_n, \quad \mathbf{a}^v = \text{Softmax}(\mathbf{v}' \mathbf{W}_v), \quad (9)$$

$$\hat{\mathbf{q}} = \sum_{n=1}^{L_v} \mathbf{a}_n^q \mathbf{q}'_n, \quad \mathbf{a}^q = \text{Softmax}(\mathbf{q}' \mathbf{W}_q), \quad (10)$$

where  $\mathbf{W}_v \in \mathbb{R}^{d \times 1}$  and  $\mathbf{W}_q \in \mathbb{R}^{d \times 1}$  are learnable matrices. Then we can compute the semantic alignment score as:

$$S(\hat{\mathbf{v}}, \hat{\mathbf{q}}) = \frac{\hat{\mathbf{v}}^T \cdot \hat{\mathbf{q}}}{\|\hat{\mathbf{v}}\|_2 \|\hat{\mathbf{q}}\|_2}, \quad (11)$$

where  $\|\cdot\|_2$  represents the L2-norm of a vector. Finally, we utilize semantic alignment scores obtained from video-query pairs in our loss term (See Section 3.5).

### 3.3.4 Decoder

We introduce the learnable spans to effectively use multimodal features in the moment prediction process, inspired by DAB-DETR [24]. Instead of naively initializing the queries with learnable embeddings as in previous work [19], we directly use moment locations as queries. We utilize learnable spans as  $S = \{S_m\}_{m=1}^M$ , and each learnable span is represented as  $S_m = (c_m, w_m)$ , where  $c_m$  and  $w_m$  refer to the center and width of the corresponding span. By doing so, learnable spans allow the model to explore various temporal locations in the video, effectively using  $X'_+$  to predict the target moment. Please refer to the Supplementary file for the implementation details.

### 3.4. Temporal Shifting

A couple of studies [12, 44, 50, 53] demonstrated that temporal augmentation techniques are effective for localization tasks. Inspired by this, we design the temporal shifting method that randomly moves the ground-truth moment to a new temporal location for our task. This allows our model to make time-equivariant predictions, but we acknowledge that this technique may disrupt long-term temporal semantic information in videos. To address this issue, we empirically apply the temporal shifting method to videos with short durations (*i.e.*,  $|V| < 60$  s). We provide a visual example with explanations in the Supplementary file.

### 3.5. Learning Objectives

**Predictions.** Based on decoder outputs, we apply MLP layers to generate a set of  $M$  predictions denoted as  $\hat{y} = \{\hat{y}_i\}_{i=1}^M$ . Each prediction  $\hat{y}_i$  contains two components: 1) the class label  $\hat{c}_i$  to indicate whether the predicted moment is the ground-truth moment or not, and 2) temporal moment location  $\hat{m}_i = (\hat{t}_s^i, \hat{t}_e^i)$ . Following the previous work [19], we find the optimal assignment  $i$  between the ground-truth  $y$  and the predictions  $\hat{y}_i$  using Hungarian algorithm based on the matching cost  $\mathcal{C}_{\text{match}}$  as:

$$\mathcal{C}_{\text{match}}(y, \hat{y}_i) = -p(\hat{c}_i) + \mathcal{L}_{\text{moment}}(m, \hat{m}_i), \quad (12)$$

$$i = \arg \min_{i \in N} \mathcal{C}_{\text{match}}(y, \hat{y}_i). \quad (13)$$

**Moment localization loss.** The moment localization loss contains two losses: 1) L1 loss and 2) a generalized IoU

Dataset	Domain	#Videos	#Queries	Avg (sec) Moment/Video	Avg Query
CharadesSTA	Activity	6.7K	16.1K	8.1 / 30.6	7.2
Anet-Cap	Activity	15K	72K	36.2 / 117.6	14.8
TACoS	Cooking	127	18K	5.4 / 287.1	10
QVHighlights	Vlog / News	10.2K	10.3K	24.6 / 150	11.3

Table 1. Statistics of VMR datasets. Avg Moment/Video denotes an average length of moment/video in seconds. Avg Query means an average number of words in query sentences.

loss [35]. This loss is designed to calculate the accuracy of a prediction by comparing it to the ground-truth moment.

$$\mathcal{L}_{\text{moment}}(m, \hat{m}_i) = \lambda_{L1} \|m - \hat{m}_i\| + \lambda_{\text{iou}} \mathcal{L}_{\text{iou}}(m, \hat{m}_i), \quad (14)$$

where  $\lambda_{L1}$  and  $\lambda_{\text{iou}}$  are the coefficients to adjust weights.

**Frame margin loss.** The margin loss encourages frames within the ground-truth moment to have high scores via hinge loss. We use a linear layer to predict the scores of the frame features  $\mathbf{f}_{\text{fore}}$  and  $\mathbf{f}_{\text{back}}$  within  $\mathbf{v}'_+$ . Note that  $\mathbf{f}_{\text{fore}}$  is located within the ground-truth moment, and  $\mathbf{f}_{\text{back}}$  is not. The loss can be formulated as follows:

$$\mathcal{L}_{\text{margin}} = \max(0, \Delta + \mathbf{f}_{\text{back}} \mathbf{W} - \mathbf{f}_{\text{fore}} \mathbf{W}), \quad (15)$$

where  $\mathbf{W} \in \mathbb{R}^{d \times 1}$ , and we set the margin  $\Delta$  as 0.2.

**Frame probability loss.** We encourage frames within the target moment to have a high probability. Let  $\mathcal{P}$  and  $\mathcal{N}$  be the sets of frame indices  $\mathbf{f}_{\text{fore}}$  and  $\mathbf{f}_{\text{back}}$ . Then we calculate the loss from the joint probability of frames  $\mathbf{p} = \{\mathbf{p}_i\}_i^{L_v}$  (in equation 6) as follows:

$$\mathcal{L}_{\text{prob}} = 1 - \frac{1}{|\mathcal{P}|} \sum_{i \in \mathcal{P}} \mathbf{p}_i + \frac{1}{|\mathcal{N}|} \sum_{j \in \mathcal{N}} \mathbf{p}_j. \quad (16)$$

**Semantic alignment loss.** We denote video-query pairs within a batch  $B$  as  $\{V_i, Q_i\}_{i=1}^N$ . We obtain multimodal features  $\{\hat{\mathbf{v}}_i, \hat{\mathbf{q}}_i\}_{i=1}^N$  and compare the semantic alignment scores (in equation 11) between positive and negative video-query pairs. The loss can be formulated as follows:

$$\mathcal{L}_{\text{semantic}} = -\frac{1}{|N|} \sum_{i=1}^N \log \frac{\exp(S(\hat{\mathbf{v}}_i, \hat{\mathbf{q}}_i)/\tau)}{\sum_{j \in \mathcal{N}} \exp(S(\hat{\mathbf{v}}_i, \hat{\mathbf{q}}_j)/\tau)}, \quad (17)$$

where  $\tau$  is a temperature parameter and set as 0.07, and  $\mathcal{N}$  means negative pairs  $\{(\hat{\mathbf{v}}_i, \hat{\mathbf{q}}_j) : i \neq j\}$ .

**Overall loss.** The overall loss is a linear combination of individual losses. Additionally, we use the class loss (*i.e.*,  $\mathcal{L}_{\text{cls}}$ ), which is the cross-entropy function computed by  $\hat{c}_i$  that classifies whether the predicted moment is the ground-truth moment. Also, we set the hyper-parameters for each loss term to adjust the scale of loss.

## 4. Experiments

### 4.1. Experiment Setup

**Datasets.** We experiment on four VMR datasets with various characteristics: Charades-STA [10], Activitynet-

Method	Feat	R@1	
		0.5	0.7
2D-TAN [54]		39.70	27.10
DRN [49]		45.40	26.40
VSLNet [51]		47.31	30.19
CBLN [23]	C3D	47.94	28.22
IVG-DCL [29]		50.24	<u>32.88</u>
MomentDiff [21]		<u>53.79</u>	30.18
BM-DETR (ours)		<b>54.08</b>	<b>34.47</b>
2D-TAN [54]		41.34	23.91
DRN [49]		42.90	23.68
CBLN [23]		43.67	24.44
FVMR [9]		42.36	24.14
SSCS [6]		43.15	25.54
UMT* [25]	VGG	48.31	29.25
MMN [42]		47.31	27.28
QD-DETR [27]		<u>52.77</u>	<u>31.13</u>
G2L [20]		47.91	28.42
MomentDiff [21]		51.94	28.25
BM-DETR (ours)		<b>56.91</b>	<b>36.24</b>
2D-TAN [54]		46.02	27.50
VSLNet [51]		42.69	24.14
MDETR [19]		53.63	31.37
QD-DETR [27]	SF+C	57.31	32.55
UniVTG [22]		<u>58.01</u>	<u>35.65</u>
MomentDiff [21]		55.57	32.42
BM-DETR (ours)		<b>59.48</b>	<b>38.33</b>

Table 2. Performance results on Charades-STA *test* split. “\*” indicates the use of additional source (*i.e.*, audio).

Captions [17] (Anet-Cap), TACoS [33], and QVHighlights [19]. We provide the statistics of datasets in Table 1.

**Implementation details.** Our model is built upon MDETR [19] implemented in Pytorch. We use the same encoder in each dataset as used in previous models: VGG [38], C3D [40], I3D [3], and SF+C, which is a concatenation of SlowFast [8] and CLIP [32]. For a fair comparison, we do not utilize negative queries or temporal shifting during inference. We provide more details in the Supplementary file.

**Evaluation metric.** We use two metrics for comparison; 1) R@n, IoU=m, which measures the percentage of the top-n predicted moments with an IoU greater than m (*e.g.*, 0.5), and 2) Mean Average Precision (mAP) over IoU thresholds.

### 4.2. Comparison with the State-of-the-Art Methods

**Baselines.** In this section, we compare BM-DETR with baselines, which can be divided into three categories: 1) traditional VMR methods that take a single query as input for predictions (*e.g.*, 2D-TAN [54]), 2) methods based on contrastive learning (*i.e.*, CL-based), including IVG-DCL [29],

Method	Feat	R@1	
		0.3	0.5
2D-TAN [54]		37.29	25.32
VSLNet [51]		29.61	24.27
DRN [49]		-	23.17
CBLN [23]		38.98	27.65
SeqPAN [52]		31.72	27.19
FVMR [9]		41.48	29.12
GTR [2]	C3D	40.39	30.22
IVG-DCL [29]		38.84	29.07
SSCS [6]		41.33	29.56
MMN [42]		39.24	26.17
G2L [20]		42.74	30.95
MomentDiff [21]		<u>44.78</u>	<u>33.68</u>
BM-DETR (ours)		<b>50.31</b>	<b>35.42</b>

Table 3. Performance results on TACoS *test* split.

Method	Feat	R@1		mAP		
		0.5	0.7	0.5	0.7	Avg.
MCN [1]		11.41	2.72	24.94	8.22	10.67
CAL [7]		25.49	11.54	23.40	7.65	9.89
XML [18]		41.83	30.35	44.63	31.73	32.14
XML+ [19]		46.69	33.46	47.89	34.67	34.90
MDETR [19]	SF+C	52.89	33.02	54.82	29.40	30.73
UMT* [25]		56.23	41.18	53.83	37.01	36.12
QD-DETR [27]		<b>62.40</b>	<b>44.98</b>	<u>62.52</u>	39.88	39.86
UniVTG [22]		58.86	40.86	57.60	35.59	35.47
MomentDiff [21]		57.42	39.66	54.02	35.73	35.95
BM-DETR (ours)		<u>60.12</u>	<u>43.05</u>	<b>63.08</b>	<b>40.18</b>	<b>40.08</b>

Table 4. Performance results on QVHighlights *test* split. “\*” indicates the use of additional source (*i.e.*, audio).

SSCS [6], MMN [42], and G2L [20], 3) methods following DETR’s detection paradigm (*i.e.*, DETR-based), including GTR [2], MDETR [19], UMT [25], QD-DETR [27], UniVTG [22], and MomentDiff [21]. In each table, the highest score is bolded, and the second highest score is underlined.

**Results on datasets.** Table 2 shows the clear superiority of BM-DETR over the baselines on Charades-STA. It is worth noting that our model shows superior performances regardless of visual feature types. TACoS and QVHighlights pose greater challenges in capturing video context since they offer longer video lengths (287s and 150s, respectively, vs 30s in Charades-STA) and diverse content such as cooking and news. Nevertheless, our model shows superior performances in Table 3 and 4. In Table 5, we observe that the performance improvement on Anet-Cap is less prominent than on the other datasets. The potential reason for this is that videos with excessive semantic overlap lead to a limited diversity of negative queries, which is more common in Anet-Cap. Although the effectiveness of our approach may diminish in such instances, our model still represents competitive results (see Section 4.5 for discussion).

Method	Feat	R@1	
		0.5	0.7
2D-TAN [54]		44.51	26.54
VSLNet [51]		43.22	26.16
DRN [49]		45.45	24.39
CBLN [23]		48.12	27.60
DeNet [57]		43.79	-
SeqPAN [52]		45.50	28.37
IVG-DCL [29]	C3D	43.84	27.10
SSCS [6]		46.67	27.56
GTR [2]		<u>50.57</u>	29.11
EMB [14]		44.81	26.07
MMN [42]		48.59	29.26
G2L [20]		<b>51.68</b>	<b>33.35</b>
BM-DETR (ours)		50.23	<u>30.88</u>

Table 5. Performance results on ActivityNet-Captions *val* split.

Method	Feat	R@1	
		0.5	0.7
2D-TAN [54]		35.88	13.91
LG [28]		42.90	19.29
DRN [49]		31.11	15.17
VSLNet [51]	I3D	34.10	17.87
DCM [45]		45.47	22.70
MDETR <sup>†</sup> [19]		46.84	19.67
Shuffling [12]		<u>46.67</u>	<u>27.08</u>
BM-DETR (ours)		<b>55.02</b>	<b>29.52</b>

Table 6. Performance results on Charades-CD *test-ood* split [48]. † indicates our reproduced results.

**Comparison with traditional VMR methods.** Our model shows superior performance across all datasets compared to traditional VMR methods, such as 2D-TAN [54], VSLNet [51]. These results indicate that accurate predictions for these methods may be challenging due to the weak alignment problem. In addition, they also easily suffer the bias problem in datasets, as we will see in the next section.

**Comparison with CL-based methods.** Our model outperforms most of the contrastive learning-based methods in Table 2, 3, and 5. Specifically, BM-DETR outperforms the recent state-of-the-art method (*i.e.*, G2L [20]) by over 7.82 points in R@1, IoU=0.7 for Charades-STA. Without incorporating complex modules like IVG module in IVG-DCL [29] or captioning objectives in SSCS [6], we simply integrate a negative query into predictions using a lightweight module (*i.e.*, PFM) consisting of only two linear layers. Additionally, unlike MMN [42] and G2L [20], which incur high computation costs associated with negative samples to improve joint representation learning, our model avoids such complexities. We quantify this in Table 10 to show the efficiency of our approach.

BMD	FS	LS	TS	R@1	
				0.5	0.7
				51.43	28.87
✓				54.73	33.28
	✓			53.76	32.13
		✓		54.39	32.23
			✓	53.47	31.12
✓	✓			55.02	33.64
✓		✓		53.98	33.53
✓			✓	54.02	33.42
✓		✓	✓	58.79	35.04
	✓	✓	✓	57.05	36.42
✓	✓	✓	✓	<b>59.48</b>	<b>38.33</b>

Table 7. Ablations on model components. We denote each model component as BMD: background-aware moment detection, FS: fine-grained semantic alignment, LS: learnable spans, and TS: temporal shifting.

$\mathcal{L}$	$\mathcal{L}_m$	$\mathcal{L}_s$	$\mathcal{L}_p$	R@1	
				0.5	0.7
				18.36	5.31
✓	✓	✓	✓	29.02	14.63
✓	✓			56.49	36.11
✓		✓		57.42	36.01
✓			✓	56.32	35.45
✓	✓		✓	58.10	36.23
✓		✓	✓	57.84	36.70
✓	✓	✓		58.68	37.59
✓	✓	✓	✓	<b>59.48</b>	<b>38.33</b>

Table 8. Ablations on losses. We denote each loss as  $\mathcal{L}$ : combination of moment localization loss and class loss,  $\mathcal{L}_m$ : frame margin loss,  $\mathcal{L}_s$ : semantic align loss, and  $\mathcal{L}_p$ : frame probability loss.

**Comparison with DETR-based methods.** Compared with the previous DETR-based methods [2, 19, 21, 22, 25, 27], our model shows competitive performance in Table 2, 3, and 4. Notably, in Charades-STA, where annotations are often weakly aligned and noisy [6, 29], our model shows a more pronounced performance improvement. This indicates that the reliance on accurate annotation of the model is reduced compared to the previous methods, validating our design choices.

### 4.3. Out-of-Distribution Testing

Charades-STA has been widely used for VMR datasets, but there are significant bias problems [31, 48] that current models heavily rely on identifying frequent patterns in the temporal moment distribution (*i.e.*, temporal bias) rather than real comprehension of multimodal inputs. To enhance evaluation reliability, we test our model on an out-of-distribution test split (*i.e.*, test-ood) where the locations of temporal moments differ from the training set. In Table 6,

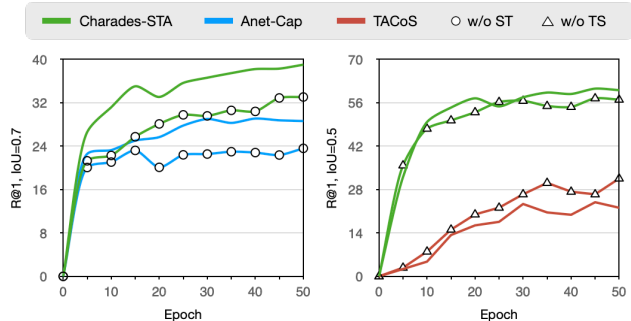


Figure 3. *Left*: Effect of sampling strategy. Bold circles indicate when our sampling strategy (ST) is not applied. *Right*: Effect of temporal shifting. Bold triangles indicate when temporal shifting (TS) is not applied.

Datasets	Neg	GT $\uparrow$	Non-GT $\downarrow$	delta $\uparrow$
Charades-STA	✓	0.42	0.20	0.22
		<b>0.56</b>	<b>0.13</b>	<b>0.43</b>
TACoS	✓	0.56	0.18	0.38
		<b>0.60</b>	<b>0.11</b>	<b>0.49</b>
Anet-Cap	✓	0.52	0.24	0.28
		<b>0.56</b>	<b>0.21</b>	<b>0.35</b>
QVHighlights	✓	0.67	0.35	0.32
		<b>0.73</b>	<b>0.28</b>	<b>0.45</b>

Table 9. The average of the joint probabilities of frames  $\mathbf{p}$  (in equation 6) inside and outside the ground-truth moment, denoted as GT and Non-GT, respectively.

Method	Iteration	Total Inference	Total Training	#GPU
MMN [42]	0.32s	37s	10h	6
G2L [20]	0.84s	43s	-	8
BM-DETR (ours)	0.19s	21s	3h	1

Table 10. Efficiency comparison on ActivityNet-Captions. The results of the other methods follow the original papers.

BM-DETR shows a remarkable performance improvement compared to the existing methods [12, 28, 45, 49, 51, 54]. While DCM [45] and Shuffling [12] are designed to address the temporal bias problem, they still follow traditional VMR methods. These results highlight the robustness of our model and re-emphasize that relying solely on a single query may be insufficient to solve the challenges in VMR.

### 4.4. Ablation Study

In this section, we conduct comprehensive ablation studies to provide an in-depth analysis of our approach.

**Ablations on model components.** To validate the effectiveness of each model component, we build up several baseline models with different model components. With the results in Table 7, we confirm that all components jointly perform well and contribute to performance improvement.

**Ablations on losses.** In Table 8, we investigate the impact of each loss.  $\mathcal{L}$  (*i.e.*,  $\mathcal{L}_{\text{cls}}$  and  $\mathcal{L}_{\text{moment}}$ ) is necessary to perform VMR as it directly guides whether the prediction matches the ground-truth. We can see that jointly combining our losses provides significant performance gains.

**Effect of sampling strategy.** In Figure 3 (*left*), we conduct experiments with and without our sampling strategy on Charades-STA and Anet-Cap. Without our sampling strategy, the model treats queries that are near the ground truth and semantically similar to target queries as negatives, resulting in significant performance degradation (around 7 points in R@1, IoU=0.7) on both datasets. This shows the importance of sampling strategy and supports that vanilla contrastive learning may be suboptimal for VMR.

**Effect of temporal shifting.** As mentioned in Section 3.4, we employ temporal shifting selectively, as it can disrupt the long-term temporal context in videos. To validate this, we conduct experiments on TACoS and Charades-STA without considering video lengths. Among the datasets used in our study, TACoS has the longest average video duration (287s), and Charades-STA has the shortest average video duration (30s). Figure 3 (*right*) shows improved performance for Charades-STA regardless of video lengths, whereas there is a decline for TACoS. This indicates that longer videos are more sensitive to our temporal shifting method, emphasizing careful usage as it could disrupt temporal information within the video and hinder training.

**Effect of using negative queries.** To study the impact of using negative queries in our modeling, we compute the average joint probability of frames  $\mathbf{p}$  (in equation 6) inside and outside the ground truth moment for each dataset. In Table 9, we can see the clear differences between using negative queries and not using them. We confirm that BM-DETR performs as intended by our design and mitigates the weak alignment problem.

**Efficiency comparison.** In Table 10, we compare the efficiency of our model with CL-based methods, including MMN [42] and G2L [20] under the same setting. While they require cumbersome computations between a number of negative video moments and queries, we can see that our model performs quite efficiently.

#### 4.5. Visualization Results

In Figure 4, we visualize our model’s predictions on videos in Charades-STA and Anet-Cap. In Charades-STA, queries typically focus on interactions between people and objects, particularly “laptops,” observed throughout the video. Our model effectively identifies and accurately predicts temporal moments for each event. For Anet-Cap, queries share similar concepts, all describing the action “dancing.” In this case, we found that our model does not treat these similar queries as negatives, even though their temporal locations differ, resulting in inaccurate predictions. This kind of issue

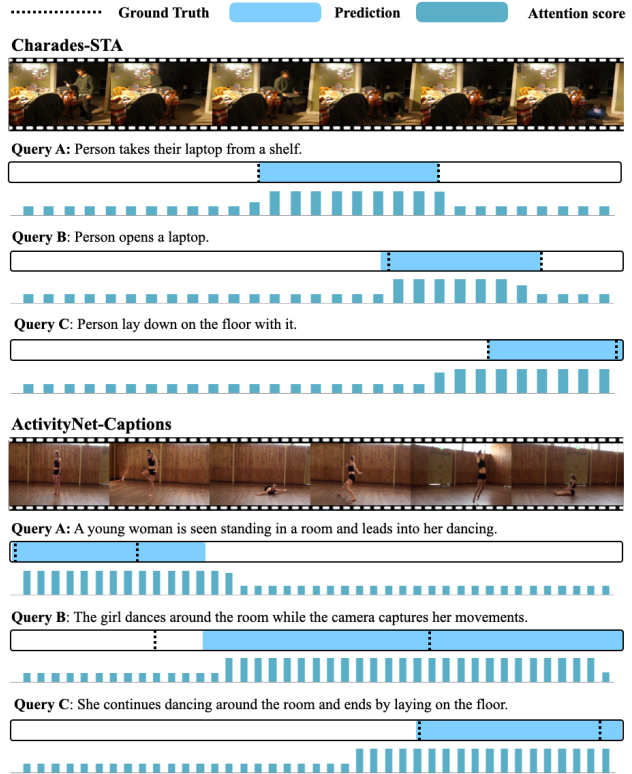


Figure 4. Visualization of predictions on videos in Charades-STA and ActivityNet-Captions. We present the attention scores (*i.e.*,  $\alpha$  in Equation 7) below the ground-truth and predicted moments.

degrades the effectiveness of our approach, and our future work will address it. More visualization results are provided in the Supplementary file.

## 5. Conclusion

In this paper, we have argued that the weak visual-textual alignment problem in videos is fatal to VMR, and present the Background-aware Moment DEtection TRansformer (BM-DETR) to alleviate it. We proposed an alternative to effectively incorporate negative queries into the moment prediction to improve overall alignments in videos while being efficient. BM-DETR achieved significant performance gains on four VMR benchmarks and even on an out-of-distribution case, highlighting its effectiveness and mitigating the weak alignment problem.

**Limitations.** One of the remaining challenges is to learn effectively even from videos with limited negative queries that can be used. Intuitively, generating diverse query sentences from video moments [15, 56] can be a potential solution. Also, there is a clear need for an algorithm that can incorporate the relationships between semantically similar queries into moment prediction. These aspects were not addressed in this study, but future work will address them and expand our method to diverse video understanding tasks.



## References

- [1] Lisa Anne Hendricks, Oliver Wang, Eli Shechtman, Josef Sivic, Trevor Darrell, and Bryan Russell. Localizing moments in video with natural language. In *Proceedings of the IEEE international conference on computer vision*, pages 5803–5812, 2017. 2, 6
- [2] Meng Cao, Long Chen, Mike Zheng Shou, Can Zhang, and Yuexian Zou. On pursuit of designing multi-modal transformer for video grounding. *arXiv preprint arXiv:2109.06085*, 2021. 2, 6, 7
- [3] Joao Carreira and Andrew Zisserman. Quo vadis, action recognition? a new model and the kinetics dataset. In *proceedings of the IEEE Conference on Computer Vision and Pattern Recognition*, pages 6299–6308, 2017. 5
- [4] Jingyuan Chen, Xinpeng Chen, Lin Ma, Zequn Jie, and Tat-Seng Chua. Temporally grounding natural sentence in video. In *Proceedings of the 2018 conference on empirical methods in natural language processing*, pages 162–171, 2018. 2
- [5] Long Chen, Chujie Lu, Siliang Tang, Jun Xiao, Dong Zhang, Chile Tan, and Xiaolin Li. Rethinking the bottom-up framework for query-based video localization. In *Proceedings of the AAAI Conference on Artificial Intelligence*, pages 10551–10558, 2020. 2
- [6] Xinpeng Ding, Nannan Wang, Shiwei Zhang, De Cheng, Xiaomeng Li, Ziyuan Huang, Mingqian Tang, and Xinbo Gao. Support-set based cross-supervision for video grounding. In *Proceedings of the IEEE/CVF International Conference on Computer Vision*, pages 11573–11582, 2021. 1, 2, 5, 6, 7
- [7] Victor Escorcia, Mattia Soldan, Josef Sivic, Bernard Ghanem, and Bryan Russell. Temporal localization of moments in video collections with natural language. *arXiv preprint arXiv:1907.12763*, 2019. 6
- [8] Christoph Feichtenhofer, Haoqi Fan, Jitendra Malik, and Kaiming He. Slowfast networks for video recognition. In *Proceedings of the IEEE/CVF international conference on computer vision*, pages 6202–6211, 2019. 5
- [9] Junyu Gao and Changsheng Xu. Fast video moment retrieval. In *Proceedings of the IEEE/CVF International Conference on Computer Vision*, pages 1523–1532, 2021. 1, 2, 5, 6
- [10] Jiyang Gao, Chen Sun, Zhenheng Yang, and Ram Nevatia. Tall: Temporal activity localization via language query. In *Proceedings of the IEEE international conference on computer vision*, pages 5267–5275, 2017. 1, 2, 5
- [11] Tengda Han, Weidi Xie, and Andrew Zisserman. Temporal alignment networks for long-term video. In *Proceedings of the IEEE/CVF Conference on Computer Vision and Pattern Recognition*, pages 2906–2916, 2022. 2
- [12] Jiachang Hao, Haifeng Sun, Pengfei Ren, Jingyu Wang, Qi Qi, and Jianxin Liao. Can shuffling video benefit temporal bias problem: A novel training framework for temporal grounding. In *Computer Vision—ECCV 2022: 17th European Conference, Tel Aviv, Israel, October 23–27, 2022, Proceedings, Part XXXVI*, pages 130–147. Springer, 2022. 4, 6, 7
- [13] Dongliang He, Xiang Zhao, Jizhou Huang, Fu Li, Xiao Liu, and Shilei Wen. Read, watch, and move: Reinforcement learning for temporally grounding natural language descriptions in videos. In *Proceedings of the AAAI Conference on Artificial Intelligence*, pages 8393–8400, 2019. 2
- [14] Jiabo Huang, Hailin Jin, Shaogang Gong, and Yang Liu. Video activity localisation with uncertainties in temporal boundary. In *European Conference on Computer Vision*, pages 724–740. Springer, 2022. 1, 2, 6
- [15] Minjoon Jung, Seongho Choi, Joochan Kim, Jin-Hwa Kim, and Byoung-Tak Zhang. Modal-specific pseudo query generation for video corpus moment retrieval. *arXiv preprint arXiv:2210.12617*, 2022. 8
- [16] Dohwan Ko, Joonmyung Choi, Juyeon Ko, Shinyeong Noh, Kyoung-Woon On, Eun-Sol Kim, and Hyunwoo J Kim. Video-text representation learning via differentiable weak temporal alignment. In *Proceedings of the IEEE/CVF Conference on Computer Vision and Pattern Recognition*, pages 5016–5025, 2022. 2
- [17] Ranjay Krishna, Kenji Hata, Frederic Ren, Li Fei-Fei, and Juan Carlos Niebles. Dense-captioning events in videos. In *Proceedings of the IEEE international conference on computer vision*, pages 706–715, 2017. 2, 5
- [18] Jie Lei, Licheng Yu, Tamara L Berg, and Mohit Bansal. Tvr: A large-scale dataset for video-subtitle moment retrieval. In *ECCV*, 2020. 6
- [19] Jie Lei, Tamara L Berg, and Mohit Bansal. Detecting moments and highlights in videos via natural language queries. *Advances in Neural Information Processing Systems*, 34: 11846–11858, 2021. 2, 4, 5, 6, 7
- [20] Hongxiang Li, Meng Cao, Xuxin Cheng, Yaowei Li, Zhihong Zhu, and Yuexian Zou. G2I: Semantically aligned and uniform video grounding via geodesic and game theory. *arXiv preprint arXiv:2307.14277*, 2023. 1, 2, 5, 6, 7, 8
- [21] Pandeng Li, Chen-Wei Xie, Hongtao Xie, Liming Zhao, Lei Zhang, Yun Zheng, Deli Zhao, and Yongdong Zhang. Momentdiff: Generative video moment retrieval from random to real. *arXiv preprint arXiv:2307.02869*, 2023. 2, 5, 6, 7
- [22] Kevin Qinghong Lin, Pengchuan Zhang, Joya Chen, Shraman Pramanick, Difei Gao, Alex Jinpeng Wang, Rui Yan, and Mike Zheng Shou. Univtq: Towards unified video-language temporal grounding. *arXiv preprint arXiv:2307.16715*, 2023. 2, 5, 6, 7
- [23] Daizong Liu, Xiaoye Qu, Jianfeng Dong, Pan Zhou, Yu Cheng, Wei Wei, Zichuan Xu, and Yulai Xie. Context-aware biaffine localizing network for temporal sentence grounding. In *Proceedings of the IEEE/CVF Conference on Computer Vision and Pattern Recognition*, pages 11235–11244, 2021. 1, 2, 5, 6
- [24] Shilong Liu, Feng Li, Hao Zhang, Xiao Yang, Xianbiao Qi, Hang Su, Jun Zhu, and Lei Zhang. Dab-detr: Dynamic anchor boxes are better queries for detr. *arXiv preprint arXiv:2201.12329*, 2022. 4
- [25] Ye Liu, Siyuan Li, Yang Wu, Chang-Wen Chen, Ying Shan, and Xiaohu Qie. Umt: Unified multi-modal transformers for joint video moment retrieval and highlight detection. In *Proceedings of the IEEE/CVF Conference on Computer Vision and Pattern Recognition*, pages 3042–3051, 2022. 2, 5, 6, 7
- [26] Antoine Miech, Jean-Baptiste Alayrac, Lucas Smaira, Ivan Laptev, Josef Sivic, and Andrew Zisserman. End-to-end

- learning of visual representations from uncurated instructional videos. In *Proceedings of the IEEE/CVF Conference on Computer Vision and Pattern Recognition*, pages 9879–9889, 2020. [2](#)
- [27] WonJun Moon, Sangeek Hyun, SangUk Park, Dongchan Park, and Jae-Pil Heo. Query-dependent video representation for moment retrieval and highlight detection. In *Proceedings of the IEEE/CVF Conference on Computer Vision and Pattern Recognition*, pages 23023–23033, 2023. [2](#), [5](#), [6](#), [7](#)
- [28] Jonghwan Mun, Minsu Cho, and Bohyung Han. Local-global video-text interactions for temporal grounding. In *Proceedings of the IEEE/CVF Conference on Computer Vision and Pattern Recognition*, pages 10810–10819, 2020. [1](#), [2](#), [6](#), [7](#)
- [29] Guoshun Nan, Rui Qiao, Yao Xiao, Jun Liu, Sicong Leng, Hao Zhang, and Wei Lu. Interventional video grounding with dual contrastive learning. In *Proceedings of the IEEE/CVF conference on computer vision and pattern recognition*, pages 2765–2775, 2021. [1](#), [2](#), [5](#), [6](#), [7](#)
- [30] Aaron van den Oord, Yazhe Li, and Oriol Vinyals. Representation learning with contrastive predictive coding. *arXiv preprint arXiv:1807.03748*, 2018. [1](#), [3](#)
- [31] Mayu Otani, Yuta Nakashima, Esa Rahtu, and Janne Heikkilä. Uncovering hidden challenges in query-based video moment retrieval. *arXiv preprint arXiv:2009.00325*, 2020. [7](#)
- [32] Alec Radford, Jong Wook Kim, Chris Hallacy, Aditya Ramesh, Gabriel Goh, Sandhini Agarwal, Girish Sastry, Amanda Askell, Pamela Mishkin, Jack Clark, et al. Learning transferable visual models from natural language supervision. In *International conference on machine learning*, pages 8748–8763. PMLR, 2021. [3](#), [5](#)
- [33] Michaela Regneri, Marcus Rohrbach, Dominikus Wetzel, Stefan Thater, Bernt Schiele, and Manfred Pinkal. Grounding action descriptions in videos. *Transactions of the Association for Computational Linguistics*, 1:25–36, 2013. [2](#), [5](#)
- [34] Nils Reimers and Iryna Gurevych. Sentence-bert: Sentence embeddings using siamese bert-networks. *arXiv preprint arXiv:1908.10084*, 2019. [3](#)
- [35] Hamid Rezatofghi, Nathan Tsoi, JunYoung Gwak, Amir Sadeghian, Ian Reid, and Silvio Savarese. Generalized intersection over union: A metric and a loss for bounding box regression. In *Proceedings of the IEEE/CVF conference on computer vision and pattern recognition*, pages 658–666, 2019. [5](#)
- [36] Cristian Rodriguez, Edison Marrese-Taylor, Fatemeh Sadat Saleh, Hongdong Li, and Stephen Gould. Proposal-free temporal moment localization of a natural-language query in video using guided attention. In *Proceedings of the IEEE/CVF winter conference on applications of computer vision*, pages 2464–2473, 2020. [2](#)
- [37] Zheng Shou, Dongang Wang, and Shih-Fu Chang. Temporal action localization in untrimmed videos via multi-stage cnns. In *Proceedings of the IEEE conference on computer vision and pattern recognition*, pages 1049–1058, 2016. [1](#)
- [38] Karen Simonyan and Andrew Zisserman. Very deep convolutional networks for large-scale image recognition. *arXiv preprint arXiv:1409.1556*, 2014. [5](#)
- [39] Surya T Tokdar and Robert E Kass. Importance sampling: a review. *Wiley Interdisciplinary Reviews: Computational Statistics*, 2(1):54–60, 2010. [3](#)
- [40] Du Tran, Lubomir Bourdev, Rob Fergus, Lorenzo Torresani, and Manohar Paluri. Learning spatiotemporal features with 3d convolutional networks. In *Proceedings of the IEEE international conference on computer vision*, pages 4489–4497, 2015. [5](#)
- [41] Ashish Vaswani, Noam Shazeer, Niki Parmar, Jakob Uszkoreit, Llion Jones, Aidan N Gomez, Łukasz Kaiser, and Illia Polosukhin. Attention is all you need. *Advances in neural information processing systems*, 30, 2017. [1](#), [3](#)
- [42] Zhenzhi Wang, Limin Wang, Tao Wu, Tianhao Li, and Gangshan Wu. Negative sample matters: A renaissance of metric learning for temporal grounding. In *Proceedings of the AAAI Conference on Artificial Intelligence*, pages 2613–2623, 2022. [1](#), [2](#), [5](#), [6](#), [7](#), [8](#)
- [43] Huijuan Xu, Kun He, Bryan A Plummer, Leonid Sigal, Stan Sclaroff, and Kate Saenko. Multilevel language and vision integration for text-to-clip retrieval. In *Proceedings of the AAAI Conference on Artificial Intelligence*, pages 9062–9069, 2019. [2](#)
- [44] Mengmeng Xu, Juan-Manuel Pérez-Rúa, Victor Escorcia, Brais Martinez, Xiatian Zhu, Li Zhang, Bernard Ghanem, and Tao Xiang. Boundary-sensitive pre-training for temporal localization in videos. In *Proceedings of the IEEE/CVF International Conference on Computer Vision*, pages 7220–7230, 2021. [4](#)
- [45] Xun Yang, Fuli Feng, Wei Ji, Meng Wang, and Tat-Seng Chua. Deconfounded video moment retrieval with causal intervention. In *Proceedings of the 44th International ACM SIGIR Conference on Research and Development in Information Retrieval*, pages 1–10, 2021. [6](#), [7](#)
- [46] Serena Yeung, Olga Russakovsky, Greg Mori, and Li Fei-Fei. End-to-end learning of action detection from frame glimpses in videos. In *Proceedings of the IEEE conference on computer vision and pattern recognition*, pages 2678–2687, 2016. [1](#)
- [47] Yitian Yuan, Tao Mei, and Wenwu Zhu. To find where you talk: Temporal sentence localization in video with attention based location regression. In *Proceedings of the AAAI Conference on Artificial Intelligence*, pages 9159–9166, 2019. [2](#)
- [48] Yitian Yuan, Xiaohan Lan, Xin Wang, Long Chen, Zhi Wang, and Wenwu Zhu. A closer look at temporal sentence grounding in videos: Dataset and metric. In *Proceedings of the 2nd International Workshop on Human-centric Multimedia Analysis*, pages 13–21, 2021. [6](#), [7](#)
- [49] Runhao Zeng, Haoming Xu, Wenbing Huang, Peihao Chen, Mingkui Tan, and Chuang Gan. Dense regression network for video grounding. In *Proceedings of the IEEE/CVF Conference on Computer Vision and Pattern Recognition*, pages 10287–10296, 2020. [1](#), [2](#), [5](#), [6](#), [7](#)
- [50] Can Zhang, Tianyu Yang, Junwu Weng, Meng Cao, Jue Wang, and Yuexian Zou. Unsupervised pre-training for

- temporal action localization tasks. In *Proceedings of the IEEE/CVF Conference on Computer Vision and Pattern Recognition*, pages 14031–14041, 2022. 4
- [51] Hao Zhang, Aixin Sun, Wei Jing, and Joey Tianyi Zhou. Span-based localizing network for natural language video localization. *arXiv preprint arXiv:2004.13931*, 2020. 1, 2, 5, 6, 7
- [52] Hao Zhang, Aixin Sun, Wei Jing, Liangli Zhen, Joey Tianyi Zhou, and Rick Siow Mong Goh. Parallel attention network with sequence matching for video grounding. *arXiv preprint arXiv:2105.08481*, 2021. 1, 2, 6
- [53] Hao Zhang, Aixin Sun, Wei Jing, and Joey Tianyi Zhou. Towards debiasing temporal sentence grounding in video. *arXiv preprint arXiv:2111.04321*, 2021. 4
- [54] Songyang Zhang, Houwen Peng, Jianlong Fu, and Jiebo Luo. Learning 2d temporal adjacent networks for moment localization with natural language. In *Proceedings of the AAAI Conference on Artificial Intelligence*, pages 12870–12877, 2020. 1, 2, 5, 6, 7
- [55] Zhu Zhang, Zhijie Lin, Zhou Zhao, and Zhenxin Xiao. Cross-modal interaction networks for query-based moment retrieval in videos. In *Proceedings of the 42nd International ACM SIGIR Conference on Research and Development in Information Retrieval*, pages 655–664, 2019. 2
- [56] Yue Zhao, Ishan Misra, Philipp Krähenbühl, and Rohit Girdhar. Learning video representations from large language models. In *Proceedings of the IEEE/CVF Conference on Computer Vision and Pattern Recognition*, pages 6586–6597, 2023. 8
- [57] Hao Zhou, Chongyang Zhang, Yan Luo, Yanjun Chen, and Chuanping Hu. Embracing uncertainty: Decoupling and de-bias for robust temporal grounding. In *Proceedings of the IEEE/CVF Conference on Computer Vision and Pattern Recognition*, pages 8445–8454, 2021. 1, 2, 6
- [58] Xizhou Zhu, Weijie Su, Lewei Lu, Bin Li, Xiaogang Wang, and Jifeng Dai. Deformable detr: Deformable transformers for end-to-end object detection. *arXiv preprint arXiv:2010.04159*, 2020. 2